JOC*Article*

Conformation of N^{α}-Substituted Hydrazino Acetamides in $CDCl_3$, the Precious Help of the Analysis of $\Delta\delta$ between Amidic Hydrogens, and Correlation to the Conformation of Aza-β^3-peptides

Arnaud Salaün,[†] Annaïck Favre,[†] Barbara Le Grel,[†] Michel Potel,[‡] and Philippe Le Grel*,[†]

SESO, UMR CNRS 6510, and Laboratoire du Solide et Inorganique Moléculaire, UMR CNRS 6511, Université de Rennes I, 263 avenue du General Leclerc CS 74205, 35042 Rennes Cedex, France

philippe.legrel@univ-rennes1.fr

Received September 8, 2005

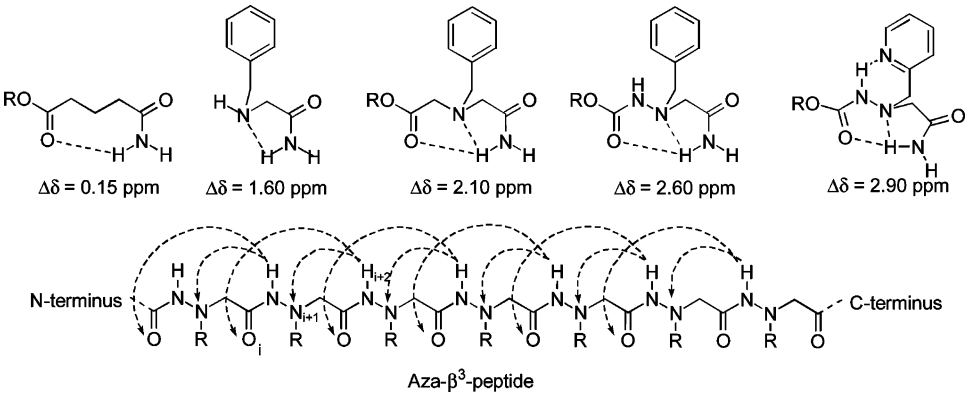

We studied the conformation of a series of primary amides in a solution of chloroform. Classical NMR tools such as dilution experiments, influence of DMSO, and 2D-NOESY, together with X-ray diffraction, were combined with an analysis of the difference of the chemical shift $\Delta\delta$ between the geminal amidic protons. This study was addressed in order to understand the conformation adopted by hydrazino acetamides **1a** and **1b** as model compounds for aza-β^3-peptides. In this manner, it was possible to show that the amidic group of these compounds acts as a H-bond donor and interacts with two different H-bond acceptors. We concluded that the hydrazinoturn, a specific bifurcated H-bond system observed in the solid state, is also the preferred conformation of hydrazino acetamides **1a** and **1b** in solution. Our results show that the short-range interaction with the N^{α}-nitrogen lone pair not only stabilizes the C8 pseudocycle but could also contribute to the folding process of aza-β^3-peptides. In light of this, it could explain why aza-β^3-peptides develop a different H-bond network in comparison to their isosteric β^3-peptides analogues. Our work is in keeping with the recent interest of hydrazino peptides as an extension of the β-peptide concept.

Introduction

α-Hydrazino acids are pseudopeptidic building blocks. Compared to the naturally occurring α-amino acids, they show an elongated backbone characterized by the presence of two adjacent nitrogen atoms (Figure 1).

Oligomerization of α-hydrazino acids leads to hydrazino peptides, which are aza-analogues of β-peptides. The latter have been shown to develop various secondary structures[1] and have originated the notion of the foldamer,[2] which refers to oligomers with discrete folding propensities. Hydrogen-bond networks are essential to the stabilization of these folded states. In aza-analogues of β-peptides, alternative H-bond networks may occur as nitrogen atoms can act as H-bond acceptors and/or H-bond donors. In this context, oligomers of α-hydrazino acids arouse a logical interest as an extension of the β-peptide concept.

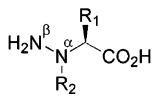

FIGURE 1. α-Hydrazino acids.

[†] SESO, UMR CNRS 6510.
[‡] Laboratoire du Solide et Inorganique Moléculaire, UMR CNRS 6511.

10.1021/jo051887q CCC: $33.50 © 2006 American Chemical Society
Published on Web 12/07/2005

In a theoretical study issued in 2001, Günther and Hofmann calculated the energies associated with the various secondary structures that could adopt oligomers of hydrazino acetic acid ($R_1 = R_2 = H$).[3] They predicted that the 3.3_{14} helix, the conformation they found the most stable, will be topologically different from the 3_{14} helix of β-peptides, because the lone pair of the N^{α} nitrogen atoms participates in its stabilization.

In 2003, Lelais and Seebach succeeded to build oligomers of optically pure α-hydrazino acids.[4] When $R_1 \neq H$ and $R_2 = H$, they obtained CD curves that resemble those of the corresponding L-β^2-peptides and suggested that this could, therefore, be indicative of the preference for a right-handed-helical secondary structure. Nevertheless, further experimental analysis of the conformation of these aza-analogues of β^2-peptides by NMR was challenging because of poor resonance dispersion and fast exchange between the NH signals. As far as we know, no definitive conclusion could have been drawn at the time.

On our side, in 2001 we published the synthesis of oligomers that are constructed exclusively with N^{α}-substituted hydrazino acetic acid ($R_1 = H$, $R_2 \neq H$).[5] Our compounds are isosteric with β^3-peptides and can be conveniently referred to as aza-β^3-peptides. L-β^3-Peptides have been shown to fold into a left-handed helical secondary structure based on 14-membered hydrogen-bonded pseudocycles.[6] In contrast, we have demonstrated that all hydrazidic NHs of aza-β^3-peptides participate in eight-membered hydrogen-bonded pseudocycles (C_8) in the opposite direction. It should be noted that such a conformation was found by Günther and Hofmann to be the second in stability behind the 3.3_{14} helix. The resulting H-bonding network induces molecular contraction but does not express into a single secondary structure, as nitrogen configuration is intrinsically uncontrolled. This means that aza-β^3-peptides must be regarded as a set of secondary structures in rapid equilibrium. Each configuration combination of the stereocenters, more precisely each diastereoisomer, gives a specific folded state. Each relies on a succession of turns. The fact remains, however, that replacing the β-carbons of β^3-peptides by nitrogen atoms fully reorganizes the H-bond network as summarized in Figure 2.

We recently obtained crystals of several aza-β^3-peptides.[7] X-ray analysis revealed that their backbones are organized by a framework of consecutive C_8 pseudocycles, reflecting the conformational preference deduced from our NMR studies in solution.[5] As crystals, each eight-membered hydrogen-bonded pseudocycle appears to be reinforced by a second internal H-bond contact with the lone pair of the previous chiral nitrogen, leading to a bifurcated H-bond. This structural feature, already observed in crystal structures of small molecular models including a single α-hydrazino acid,[8] is referred to as hydrazinoturn (Figure 3). Similar models including a single α-aminoxy acid, where an oxygen atom replaces the NR_1 group, show almost the same arrangement.[9]

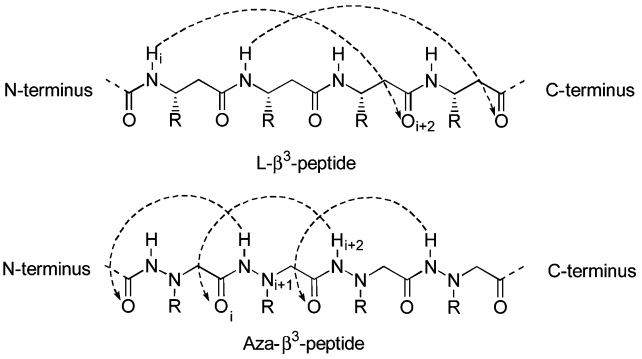

FIGURE 2. Comparison of the H-bond network in β^3-peptides and aza-β^3-peptides.

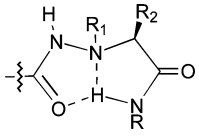

FIGURE 3. Hydrazinoturn.

These characteristics observed in the solid state, as well as the theoretical calculation by Günther and Hofmann, question the actual contribution of the lone pair of the pyramidal nitrogen center as an H-bond acceptor to stabilize the secondary structure of hydrazino peptides. In particular, does such an interaction really contribute to stabilize the conformation of aza-β^3-peptides in solution? To our knowledge, such an interaction has never been experimentally demonstrated. We describe here that the careful analysis of the chemical shift differences $\Delta\delta$ between geminal amidic hydrogen is helpful to solve this challenging problem. This structural approach, combined with classical NMR tools, allowed us to fully elucidate the conformational preference of N^{α}-substituted hydrazino acetamides. Our findings lead us to propose an explanation in order to rationalize the radically different H-bond network developed by β^3-peptides and aza-β^3-peptides.

Results and Discussion

The present work began with the observation that the chemical shift difference, $\Delta\delta$, between the two amidic protons

(1) (a) Seebach, D.; Beck, A. K.; Bierbaum, D. J. *Chem. Biodiversity* **2004**, *1*, 1111. (b) Appela, D. H.; Christianson, L. A.; Klein, D. A.; Powell, D. R.; Huang, X.; Barchi, J. J., Jr.; Gellman, S. H. *Nature* **1997**, *387*, 381. (c) Appela, D. H.; Christianson, L. A.; Karle, I. L.; Powell, D. R.; Gellman, S. H. *J. Am. Chem. Soc*. **1999**, *121*, 6206. (d) Appela, D. H.; Christianson, L. A.; Klein, D. A.; Richards, M. R.; Powell, D. R.; Gellman, S. H. *J. Am. Chem. Soc*. **1999**, *121*, 7574. (e) Barchi, J. J., Jr.; Huang, X.; Appela, D. H.; Christianson, L. A.; Durell, S. R.; Gellman, S. H. *J. Am. Chem. Soc*. **2000**, *122*, 2711.

(2) (a) Gellman, S. H. *Acc. Chem. Res*. **1998**, *31*, 173. (b) Hill, D. J.; Mio, M. J.; Prince, R. B.; Hughes, T. S.; Moore, J. S. *Chem. Rev*. **2001**, *101*, 3893.

(3) Günther, R.; Hofmann, H.-J. *J. Am. Chem. Soc*. **2001**, *123*, 247.

(4) Lelais, G.; Seebach, D. *Helv. Chim. Acta* **2003**, *86*, 4152.

(5) Cheguillaume, A.; Salaün, A.; Sinbandhit, S.; Potel, M.; Gall, P.; Baudy-Floc'h, M.; Le Grel, P. *J. Org. Chem.* **2001**, *66*, 4923.

(6) (a) Seebach, D.; Overhand, M.; Kühnle, F. N. M.; Martinoni, B.; Oberer, L.; Hommel, U.; Widmer, H. *Helv. Chim. Acta* **1996**, *79*, 913. (b) Seebach, D.; Ciceri, P. E.; Overhand, M.; Jaun, B.; Rigo, D.; Oberer, L.; Hommel, U.; Amstutz, R.; Widmer, H. *Helv. Chim. Acta* **1996**, *79*, 2043. (c) Seebach, D.; Abele, S.; Gademann, K.; Guichard, G.; Hintermann, T.; Jaun, B.; Matthews, J. L.; Schreiber, J. V.; Oberer, L.; Hommel, U.; Widmer, H. *Helv. Chim. Acta* **1998**, *81*, 932.

(7) Salaün, A.; Potel, M.;Roisnel, T.; Gall, P.; Le Grel, P. *J. Org. Chem.* **2005**, *70*, 6499;

(8) (a) Aubry, A.; Bayeul, D.; Mangeot, J.-P.; Vidal, J.; Sterin, S.; Collet, A.; Lecoq, A.; Marraud, M. *Biopolymers* **1991**, *31*, 793. (b) Marraud, M.; Dupont, V.; Grand, V.; Zerkout, S.; Lelocq, A.; Boussard, G.; Vidal, J.; Collet, A.; Aubry, A. *Biopolymers* **1993**, *33*, 1135. (c) Aubry, A.; Mangeot, J.-P.; Vidal, J.; Collet, A.; Zerkout, S.; Maraud, M. *Int. J. Pept. Protein Res*. **1994**, *43*, 305. (d) Zerkout, S.; Dupont, V.; Aubry, A.; Vidal, J.; Collet, A.; Vicherat, A.; Marraud, M. *Int. J. Pept. Protein Res*. **1994**, *44*, 378.

(9) (a) Yang, D.; Qu, J.; Li, B.; Ng, F.-F.; Wang, X.-C.; Cheung, K.-K.; Wang, D.-P.; Wu, Y.-D. *J. Am. Chem. Soc*. **1999**, *121*, 589. (b) Thevenet, L.; Vanderesse, R.; Marraud, M.; Didierjean, C.; Aubry, A. *Tetrahedron Lett*. **2000**, *41*, 2361. (c) Yang, D.; Li, B.; Ng, F.-F.; Yan, Y.-L.; Qu, J.; Wu, Y.-D. *J. Org. Chem.* **2001**, *66*, 7303.

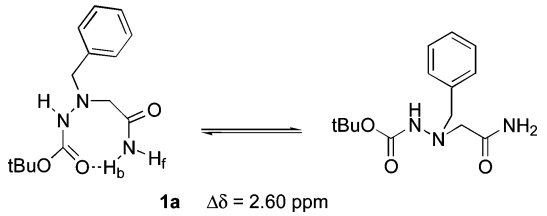

FIGURE 4. Discrimination of amidic protons through H-bonding.

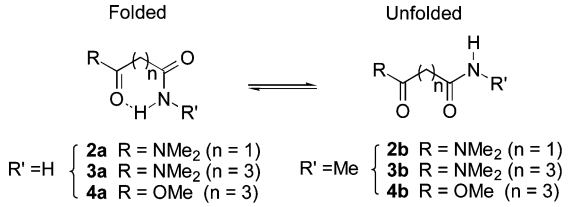

FIGURE 5. Equilibrium between the folded and unfolded state relying on an intramolecular H-bond in bifunctional homologous alkanes.

of compound **1a** (10 mM in $CDCl_3$) was revealed to be unusually large ($\Delta\delta = 2.60$ ppm). As compound **1a** can be regarded as a general model for aza-β^3-peptides, we assumed that the high $\Delta\delta$ observed must be related to the fact that the amide group belongs to an eight-membered hydrogen-bonded pseudocycle.

Indeed, as represented in Figure 4, H-bonding is prone to slow the rotation about the N−CO bond and should therefore discriminate the two geminal amidic protons by increasing the chemical shift of the bonded NH (NH_b) relative to the "free" one (NH_f). As an empirical rule one can assume that the $\Delta\delta$ value will be greater when the equilibrium is shifted toward the hydrogen-bonded state.

To further verify our hypothesis, we took advantage of a work by Gellman,[10] who studied the equilibrium between the hydrogen-bonded state (folded state) and the non-hydrogen-bonded state (unfolded state) for a series of homologous secondary amides, which display variable sizes of potential hydrogen-bonded pseudocycles (Figure 5).

His conclusions, mostly based on VT-IR experiments, were made possible because the judiciously chosen models displayed a single NH vibrator. This study demonstrated that if compounds **2b** and **3b** both equilibrate between the hydrogen-bonded and non-hydrogen-bonded states, **2b** predominantly occurs in the folded state (C_6) while **3b** largely prefers the unfolded state (C_8). In contrast, there was no evidence of the folded state (C_8) in the case of compound **4b**, whose much less polarized ester group is a poor hydrogen bond acceptor.

We synthesized the primary amide analogues **2a**, **3a**, and **4a** assuming that, at low concentration, they should behave like the corresponding secondary amides (Figure 5). The $\Delta\delta$ values were measured and compared with the results of Gellman.

^{1}H NMR spectra were run in $CDCl_3$ at different concentrations. In every case, the amidic NHs appear as two distinct signals of equal intensity. To simplify the discussion, we will use NH_f to refer to the higher field signal and NH_b to refer to the lower field signal, although it is clear that both folded and unfolded states contribute to the resonance.

We observed that the $\Delta\delta$ values are no longer significantly affected under 10 mM, indicating that from this dilution the influence of intermolecular H-bonding on chemical shifts is negligible. Consequently, all of the $\Delta\delta$ discussed in this paper have been measured at this concentration. Taking into account that the concentration could be controlled only with a limited precision, the $\Delta\delta$ values are rounded within 0.05 ppm.

$\Delta\delta$ values of compounds **2a**, **3a**, and **4a** are, respectively, 2.30, 0.70, and 0.15 ppm. These values are in excellent qualitative agreement with Gellman's conclusions since they vary in the expected way. The much larger value observed for **2a** in comparison with **3a** is coherent with the important displacement of the equilibrium toward the six-membered pseudocyclic folded state. In the case of **2a**, increasing the concentration from 10 to 100 mM, therefore favoring intermolecular H-bonding, shifts H_f significantly downfield (+0.26 ppm) while H_b is almost unaffected (−0.03 ppm) (Figure 6a). The same tendency is observed when increasing amounts of DMSO-d_6 are added (Figure 6b).

For **3a**, both NHs move downfield, confirming that in this case the unfolded state is predominantly populated (Figure 6c and d).

Contrary to the fact that no folded state was detected in the IR spectrum of **4b**, $\Delta\delta$ of **4a** is very low but not null. This suggests that the NH_2 group should still be able to experience a H-bond contact with the ester group. To verify if steric hindrance alone could differentiate the two amidic protons, we prepared the sterically comparable 4-phenylbutyramid **5** (Figure 7), in which no significant H-bond acceptor is present.[11] $\Delta\delta$ of **5** is null. This means that although the extinction coefficient of the hydrogen-bonded state of **4b** is too small to observe its IR absorption at low concentration, $\Delta\delta$ of the related compound **4a** reveals that a very weak interaction nevertheless occurs.

From this preliminary work we concluded that $\Delta\delta$ analysis is a valuable and highly sensitive tool to detect the intramolecular hydrogen bond interaction of a primary amide group as an H-bond donor. With this new tool in hand, we turned to explore the conformation of N^{α}-substituted hydrazino acetamides.

Applying $\Delta\delta$ to the Analysis of the Conformational Behavior of Hydrazino Acetamides. In comparison with compound **4a** ($\Delta\delta = 0.15$ ppm), the hydrazino acetamide **1a** reveals a much higher $\Delta\delta$ value ($\Delta\delta = 2.60$ ppm). Since both compounds fold into eight-membered hydrogen-bonded pseudocycles, the value of **1a** implies that specific structural features must be present, displacing the equilibrium toward the folded state. To determine the different parameters that could contribute to the $\Delta\delta$ observed for this compound, we synthesized a series of selected primary amides and attempted to rationalize the evolution of the corresponding $\Delta\delta$. In this manner, we anticipate that it should be possible to evaluate the influence of an eventual H-bond interaction between the amide group and the nitrogen lone pair of the N^{α} nitrogen atom on the $\Delta\delta$ (Figure 8) as suggested by the above X-ray data.

In contrast with compound **5**, the $\Delta\delta$ value of the isosteric amide **6a** is 1.60 ppm (Figure 9). $\Delta\delta$ of the upper homologue **7** is 2.15 ppm. A strong anisotropic effect by the phenyl ring on the $\Delta\delta$ value observed for **6a** or **7** can be eliminated as $\Delta\delta$ is 1.75 ppm for **6b**. A quantitative comparison between these values and that of **2a** or **3a** should be used with cautious since

(10) Gellman, S. H.; Dado, G. P.; Liang, G.-B.; Adams, B. R. *J. Am. Chem. Soc.* **1991**, *113*, 1164.

(11) H-bonding with aromatic π-system is nevertheless possible and such interactions, commonly encountered in proteins, was reviewed recently: Meyer, E. A.; Castellano, R. K.; Diederich, F. *Angew. Chem., Int. Ed.* **2003**, *42*, 1210.

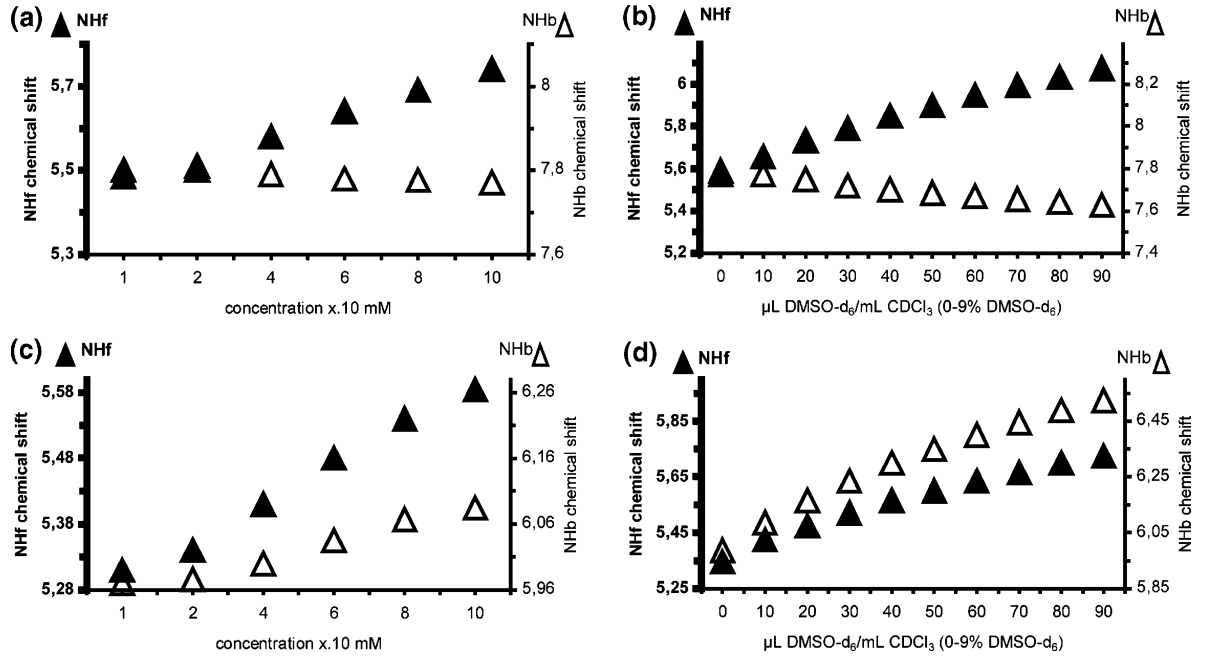

FIGURE 6. (*a*) NH chemical shifts of **2a** as a function of its concentration in $CDCl_3$. (b) NH chemical shifts of **2a** (20 mM) as a function of the concentration of DMSO-d_6. (c) NH chemical shifts of **3a** as a function of its concentration in $CDCl_3$. (d) NH chemical shifts of **3a** (20 mM) as a function of the concentration of DMSO-d_6.

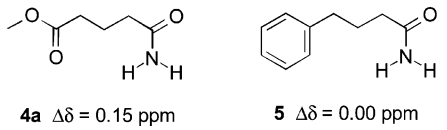

FIGURE 7. $\Delta\delta$ values for the sterically comparable amides **4a** and **5**.

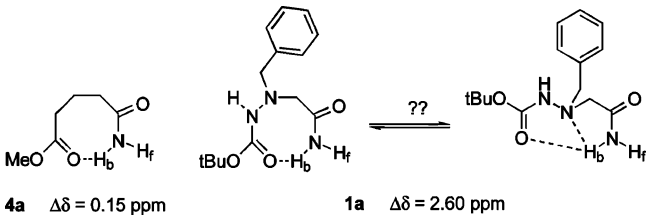

FIGURE 8. Possible influence of the sp^3 nitrogen lone pair to the $\Delta\delta$.

the nature of the hydrogen bond acceptors and the geometry of the hydrogen bonds differ. Nevertheless, it is clear that the primary amides of **6a** and **6b** substantially interact with the lone pair of the sp^3 nitrogen. This is also confirmed by the DMSO experiments where the NH_b remains almost unaffected (+0.03 ppm). The resulting H-bond gives rise to a five-membered hydrogen-bonded pseudocycle.

The information derived from the $\Delta\delta$ analysis appears in the solid state as **6a** crystallizes in a trimeric system, where each molecule, although making intermolecular contact through the amide group, is internally H-bonded with the lone pair of the sp^3 nitrogen atom ($N^{\alpha}\cdots H_b$ = 2.32 Å) as postulated (Figure 10).

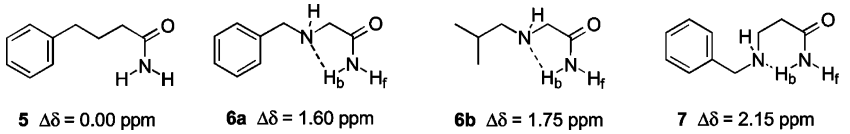

FIGURE 9. Comparison of $\Delta\delta$ in a series of α-amino amides.

Tertiary Amines Bearing Both H-Bond Donor and H-Bond Acceptor. The tertiary amine **8b** combines the structural features present in compounds **3a** and **6a** (Figure 11). The $\Delta\delta$ value of **8b** (2.60 ppm) is higher than the sum of the individual values (0.70 + 1.60). By assuming that compound **8b** can adopt a bifidic folded state, the nonlinearity observed can be interpreted as the result of a more favorable entropic situation. In such a conformation, the two H-bond acceptors, although competitive, mutually reinforce their efficiencies by restraining the flexibility of the molecule. Considering the respective $\Delta\delta$ value of **3a** and **6a**, it is reasonable to propose that the five-membered hydrogen-bonded pseudocycle is the most important contributor to the folding process, since its most favorable formation makes the subsequent participation of the carbonyl group easier. This is confirmed by $\Delta\delta$ value of compound **8a**, which reaches 2.10 ppm, despite the presence of the significantly less polarized ester group. For the symmetrical compound **8c**, the $\Delta\delta$ value (1.20 ppm) is about half of the value of compound **8b** (2.60 ppm). This is quite logical since each amid group alternatively acts as H-bond donors and H-bond acceptors. The small deviation between the experimental value (1.20 ppm) and the expected value (1.30 ppm) most likely arises from the difference in polarity between primary and tertiary amides.

***N*$^{\alpha}$-Benzyl-hydrazino Acetamide 1a and 1b.** Replacing the methylene fragment of **8a** or **8b** by a NH group introduces a new H-bond donor. The six-membered hydrogen-bonded pseudocycle could compete with the bifidic arrangement (Figure 12). However, since this NH is actually very sensitive to the addition of DMSO and since the aza-analogues **1a** ($\Delta\delta$ = 2.60

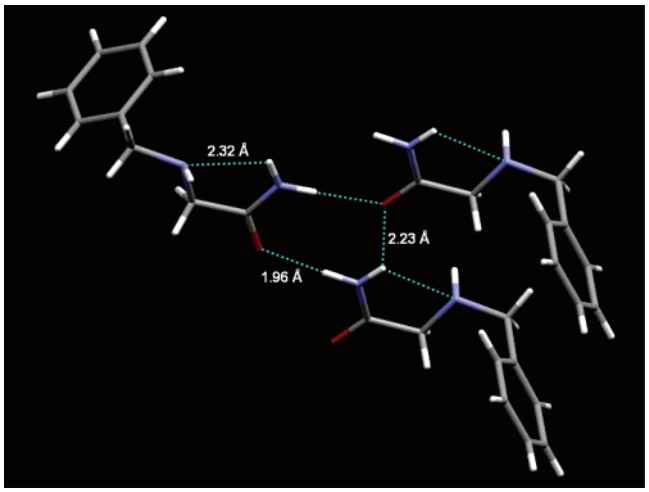

FIGURE 10. X-ray crystal structure of **6a**. H-bond distances are given in angstroms.

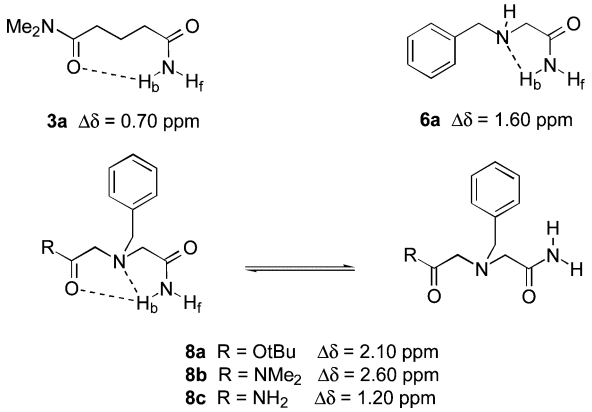

FIGURE 11. Comparison of $\Delta\delta$ values between various disubstituted amines.

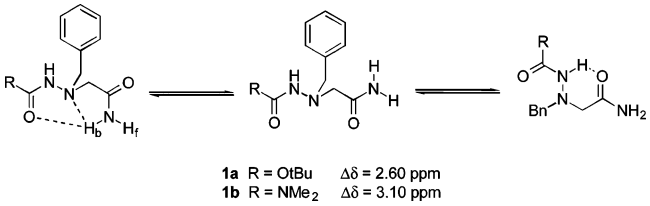

FIGURE 12. Potential conformations of N^{α}-benzyl-hydrazino acetamide **1a** and **1b**.

ppm) and **1b** ($\Delta\delta$ = 3.10 ppm) show higher $\Delta\delta$ values with respect to compounds **8a** and **8b**, both of these facts argue against a significant population of a C_6 conformation.

The gain of 0.50 ppm observed for N^{α}-substituted hydrazino acetamides **1a** and **1b** reveals a greater propensity to stabilize the bifidic arrangement. We assume that this is in relation to the lone-pair electron repulsion in the N−N fragment. This structural constraint is known to favor an orthogonal arrangement between the lone pairs.[12] In this sense, to some extent, it restrains the flexibility of the hydrazino fragment, acting as a type of braking mechanism toward the rotation about the N−N bond. When rotation occurs, lone pairs tend to eclipse and electronic repulsion increases. Part of the repulsion will be released if the N^{β} lone pair conjugates efficiently with the adjacent carbonyl group. The latter will become more polarized, thus making it a stronger H-bond acceptor. This phenomenon most likely occurs because both methyl groups are magnetically equivalent for **1b**, even though they give two distinct singlets in the case of **8b**, attesting to the fact that the N^{β} lone pair is competitive with the powerful electron-releasing dimethylamino group (Figure 13).

(12) Dewar, M. J. S.; Jennings, W. B. *J. Am. Chem. Soc.* **1973**, *95*, 1562.

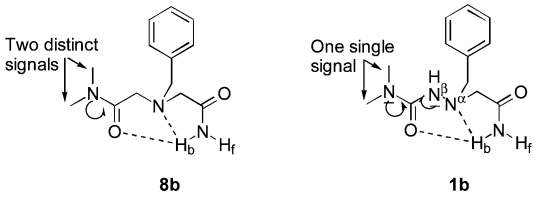

FIGURE 13. ^{1}H NMR resonance of dimethylamino group in **8b** and **1b**.

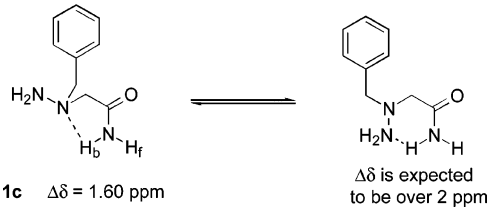

FIGURE 14. Possible H-bond interactions between amidic and hydrazino fragments.

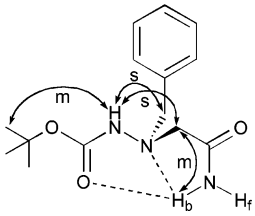

FIGURE 15. Summary of the NOEs observed for **1a** (20 mM in $CDCl_3$).

The $\Delta\delta$ value of the unprotected compound **1c** drops down to 1.60 ppm. This brings forth two important points. First of all, it further confirms the contribution of the carbonyl group to the $\Delta\delta$ in **1a**. Second, it is also indicative of a substantial interaction between the hydrazino moiety and the amidic hydrogen (Figure 14). Both five-membered and six-membered conformations could contribute to the folding process in a competitive way. As the $\Delta\delta$ value of **1c** is closer to that of **6a** (1.60 ppm) than to that of **7** (2.15 ppm), it seems to indicate a preference for a five-membered hydrogen-bonded conformation. This could, however, be related to the fact that the lone-pair electron repulsion could be more easily assumed with an exocyclic terminal nitrogen, yet this last point remains conjectural.

2D-NOESY spectrum of compound **1a** was recorded. The principal NOEs observed are represented in Figure 15. NOE is clearly observed between the carbazidic NH and the *tert*-butyl fragment. This implies that the carbazidic bond is substantially retained in the *Z* geometry. Strong NOE is also observed between both methylenes and the carbazidic NH. Consequently, the carbazidic NH is oriented toward these groups in the major conformation. No NOE can be detected for NH_f. In contrast, NOE is observed between NH_b and the methylene protons of the acetamide chain. As postulated, this strong discrimination

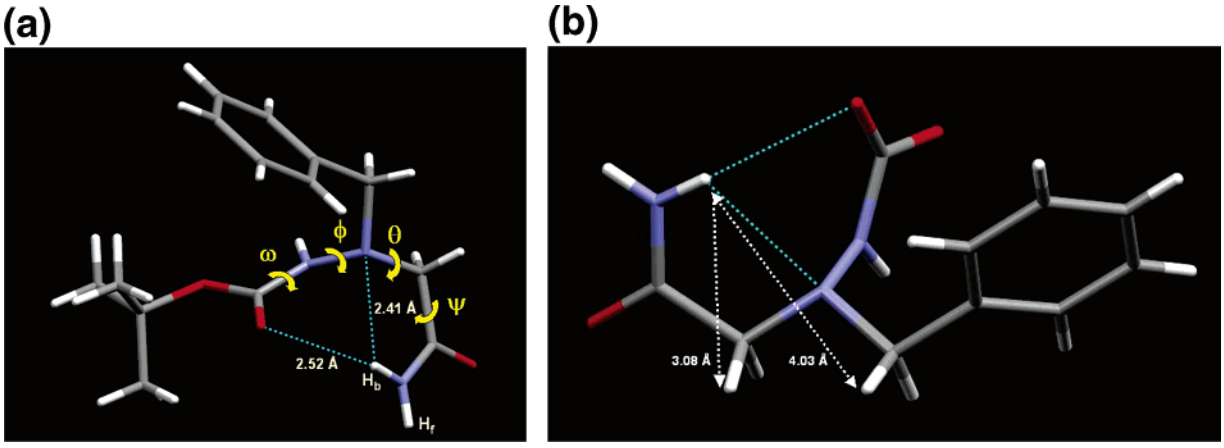

FIGURE 16. (a) X-ray crystal structure of **1a** bond length and torsional angles. (b) Distances between NH_b and methylenic showing H-protons. The *t*Bu group is omitted for clarity.

TABLE 1. Torsional Angles of (*R*)- and (*S*)-Hydrazinoturn for Compound 1a

	torsional angle (deg)			
	ω	ϕ	θ	ψ
(*R*)-hydrazinoturn	+163	+133	−75	−14
(*S*)-hydrazinoturn	−163	−133	+75	+14

between the NOEs of the two amidic NHs is easily explained by the positioning of the amide group during its interaction with the lone pair of the chiral nitrogen center. It is also important to point out that only a very weak NOE is observed between NH_b and the benzylic methylene. This is consistent with the H-bonding of NH_b with the lone pair of the chiral nitrogen, since this interaction forcibly displaces it away from the benzylic chain.

We obtained suitable crystals of compound **1a** as a racemate. X-ray diffraction revealed a hydrazinoturn-type arrangement, which perfectly correlates to the conformation proposed from the study in solution (Figure 16a). One of the amidic protons is H-bonded with both the lone pair of the sp^3 nitrogen atom ($N^{\alpha}\cdots HN = 2.41$ Å) and the oxygen of the carbazidic group ($CO\cdots HN = 2.52$ Å). Figure 16b shows that the hydrazinoturn arrangement concomitantly moves the H-bonded hydrogen atom closer to the acetamidic methylene ($NH\cdots CH \approx 3$ Å) and away from the benzylic protons ($NH\cdots CH \approx 4$ Å) as expected.

On Figure 16a we have represented the four torsional angles ω, ϕ, θ, and ψ, which characterize a hydrazinoturn. The values measured for a (*R*)-hydrazinoturn and a (*S*)-hydrazinoturn[13] in compound **1a** are listed in Table 1. The slight pyramidalization of the N^{β} nitrogen atom induces a small deviation of ω from the ideal value expected for the *Z* geometry of the carbazidic linkage. The value of the torsional angle ϕ permits the lone pair of electrons of the two adjacent nitrogen atoms to adopt an orthogonal arrangement (Figure 17a). The values taken by θ (around −75° or +75°), which are imposed by H-bonding with the amide group, correspond to a (−)-synclinal or (+)-synclinal conformation. This places the R_2 substituent in a favorable free zone of space (Figure 17b). The values of ω, ϕ, and θ are similar to those that are observed in the L-β^3-peptides. In contrast, resulting from the existence of the H-bond between NH_b and the N^{α} nitrogen atom (Figure 17c), the value of ψ radically differs from the corresponding angles in the L-β^3-peptides,[1a] which are around −140°. This interaction appears pivotal in the divergence of the H-bond networks between the L-β^3-peptides and our aza-analogues. The above structural features associated with these sets of angles permit us to conclude that the hydrazinoturn conformation allows the simultaneous minimizing of both steric crowding and electronic repulsion.

(13) (*R*)- or (*S*)-Hydrazinoturn refer to the corresponding absolute configuration of the N^{α} nitrogen atom.

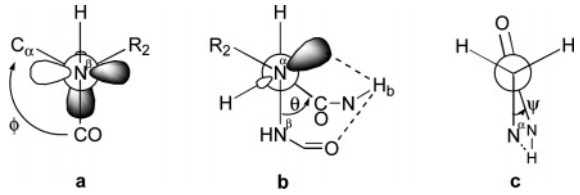

FIGURE 17. Schematic Newman projections illustrating the structural features in relationship to angles ϕ, θ, and ψ for a (*R*)-hydrazinoturn.

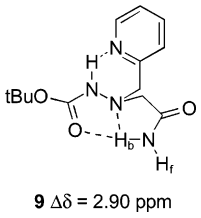

9 $\Delta\delta$ = 2.90 ppm

FIGURE 18. H-bond network for compound **9**.

As a final illustration of the sensitivity of the $\Delta\delta$ value to small structural variations, we also synthesized compound **9** where the phenyl ring of **1a** is replaced by a 2-pyridyl ring. In this compound the $\Delta\delta$ value is slightly higher (2.90 ppm) than in **1a** (2.60 ppm), while the carbazidic NH is shifted to lower field (7.41 versus 5.67 ppm**)**. The latter is clearly H-bonded with the nitrogen atom of the pyridyl ring. This extra interaction, by reducing further the rotation around the carbazidic linkage, leads to a logical increase of the $\Delta\delta$ value as a result of the cooperative effect. The resulting conformation represented in Figure 18 allows the pairing of most potential H-bond partners.

Conclusions

A hydrazinoturn, where an H-bond donor equilibrates between two H-bond acceptors, is the preferred conformation of N^{α}-substituted hydrazino acetamides in solution.

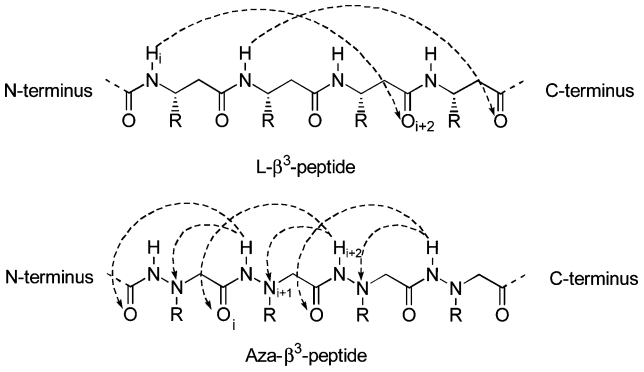

FIGURE 19. Differences between H-bond networks of β^3-peptides and aza-β^3-peptides.

The H-bond interaction between the lone pair of the chiral nitrogen atom and the amidic hydrogen atom stabilizes the hydrazinoturn conformation but also participates during the folding process. Our results suggest that this short-range interaction could help the C8 pseudocycle to form by preorganizing the hydrazino fragment in a way that favors further H-bonding with the carbonyl group. Consequently, this interaction contribute appreciably in the divergence of the H-bond network developed by our aza-β^3-peptides and the corresponding β^3-peptides (Figure 19).

Once organized, the hydrazinoturn conformation is efficiently maintained by the cooperativity of the two H-bond acceptors and the lone-pair electron repulsion between the two adjacent nitrogen atoms.

Although particularly favored for N^{α}-substituted hydrazino acetamides, such a bifurcated conformation is also significantly populated in the case of suitably substituted tertiary amines (compounds **8a**−**c**).

To some extent, our experimental findings correlate to the theoretical study by Günther and Hofmann, who predicted that the N^{α} nitrogen lone pair in oligomers of hydrazino acetic acid should contribute to the stabilization of the lowest-energy secondary structures as an H-bond acceptor. On the other hand, these authors predicted these interactions to be less important than the contact of the NH to CO groups. Our study suggests that, in the case of aza-β^3-peptides, the N^{α} nitrogen atoms play an important role both in the dynamics of the folding process and the stabilization of the folded state.

Our conclusions were made possible by comparing the difference of the chemical shift $\Delta\delta$ between the geminal hydrogen atoms of the primary amide group. This spectral data, which revealed a very sensitive H-bond sensor, is a valuable alternative in the exploration of intramolecular H-bonded systems. IR spectroscopy is of limited interest in this case because of the overlapping of individual absorptions. In a final analysis, it is important to note that even if the $\Delta\delta$ values mostly result from the equilibrium between the folded and the unfolded state, it is not easy to quantify the contribution of the nature of the H-bond acceptor and the geometry of the H-bond interaction. For example, one can reasonably consider that the geometry of the H-bond is similar for compounds **2a** and **7**, which both fold into six-membered pseudocycle. However, to what extent does the magnetic anisotropy induced by the carbonyl group influence the chemical shift of the H-bonded hydrogen? On the other hand, the H-bond acceptor is the same for compound **6a**, and **7**, but the geometry of the H-bond in the respective five-membered and six-membered pseudocycles obviously differ. To what extent does this parameter influence the $\Delta\delta$? As this value is clearly sensitive to small structural variations, we hope that it could be further exploited to go deeper in the understanding of the H-bond interaction in a more general context.

Experimental Section

***N*$^{\alpha}$-Benzyl,*N*$^{\beta}$-Boc Hydrazino Acetamide (1a).** Compound **1a** was obtained from the corresponding N^{α}-benzyl,N^{β}-Boc hydrazino acetic methyl ester that was ammonolyzed quantitatively in 24 h (following general procedure described in Supporting Information). Evaporation of NH_3/MeOH directly afforded a white powder. Monocrystals of N^{α}-benzyl,N^{β}-Boc hydrazino acetamide were grown from CH_3CN: mp 185 °C; ^{1}H NMR 500 MHz (10 mM, $CDCl_3$) δ 1.39 (s, 9H, 3xCH_3), 3.40 (s, 2H, CH_2), 3.98 (s, 2H, CH_2), 5.40 (broad, 1H, NH), 5,67 (1H, carbazidic NH), 7.33 to 7.38 (m, 5H, aromatics), 8.00 (broad, 1H, NH). Anal. Calcd: C, 60.20; H, 7.58; N, 15.04. Found: C, 60.51; H, 7.62; N, 15.17.

***N*$^{\alpha}$-Benzyl Hydrazino Acetamide (1c).** Compound **1a** (2 g; 7.17 mmol) was dissolved into CH_2Cl_2/TFA (10 mL/6 mL). The solution was kept standing for 3 h. Then, 30 mL CH_2Cl_2 and 10 mL water were added and the medium was neutralized by addition of solid $NaHCO_3$ under vigorous stirring. The compounds was extracted twice with 20 mL of EtOAc. After drying the combined organic layers on Na_2SO_4, evaporation afforded crude N^{α}-benzyl hydrazino acetamide (0.84 g, 65%): ^{1}H NMR 200 MHz (10 mM, $CDCl_3$) δ 3.08 (broad, 2H, NH_2), 3.30 (s, 2H, CH_2), 3.79 (s, 2H, CH_2), 5.45 (broad, 1H, NH), 7.05 (broad, 1H, NH), 7.29 to 7.42 (m, 5H, aromatics).

***N*$^{\alpha}$-Benzyl,*N*$^{\beta}$-dimethylcarbamoyl Hydrazino Acetamide (1b).** Compound **1c** (0.50 g; 2.79 mmol), triethylamine (0.34 g; 3.35 mmol), and 0.36 g of *N*,*N*-dimethyl carbamoyl chloride (3.35 mmol) were dissolved into 10 mL of CH_3CN. The solution was refluxed in an oil bath for 2 h. Then 30 mL of CH_2Cl_2 was added and the organic layer was successively washed with 20 mL of 1 N HCl and 20 mL of 1 M $NaHCO_3$ and finally dried on Na_2SO_4 before evaporation. The residue was dissolved into EtOAc, and the solution, refrigerated, afforded N^{α}-benzyl,N^{β}-dimethylcarbamoyl hydrazino acetamide as a white powder (0.20 g, 29%): mp 165−167 °C; ^{1}H NMR 500 MHz (10 mM, $CDCl_3$) δ 2.87 (s, 6H, $N(CH_3)_2$), 3.45 (s, 2H, CH_2), 4.04 (s, 2H, CH_2), 5.40 (broad, 1H, NH), 5.74 (broad, 1H, NH), 7.34 to 7.41 (m, 5H, aromatics), 8.50 (broad, 1H, NH). Anal. Calcd: C, 57.58; H, 7.25; N, 22.38. Found: C, 57.25; H, 7.14; N, 22.11.

***N*,*N*-Dimethylpropane Diamide (2a).** The mono-*N*,*N*-dimethylamide of malonic acid was prepared following Gellman's procedure.[10]

To 2.80 g (21 mmol) of that crude compound in 30 mL of MeOH cooled to −10 °C was added dropwise a solution of 3.80 g (32 mmol) of thionyl chloride in 20 mL of CH_2Cl_2.The solution was then allowed to warm to room temperature and stirred for further 1 h. Solvents were then evaporated, and the crude resulting oil was dissolved in 30 mL of CH_2Cl_2. The organic layer was washed twice with 30 mL of 1 M $NaHCO_3$, dried over Na_2SO_4, and evaporated to give 2.50 g (81%) of the corresponding malonic methyl ester: ^{1}H NMR 200 MHz ($CDCl_3$) δ 3.01 (s, 3H, NCH_3), 3.07 (s, 3H, NCH_3), 3.50 (s, 2H, CH_2), 3.79 (s, 3H, OCH_3). This material was carried on without further purification.

Ammonolysis was performed in 48 h following the general procedure described in Supporting Information. Dissolving the crude yellow oil in Et_2O directly afforded pure *N*,*N*-Dimethylpropane diamide **2a** as an off-white solid (0.41 g, 19%): mp 128−129 °C; ^{1}H NMR 500 MHz (10 mM, $CDCl_3$) δ 3.02 (s, 3H, NCH_3), 3.11 (s, 3H, NCH_3), 3.36 (s, 2H, CH_2), 5.50 (broad, 1H, NH), 7.80 (broad, 1H, NH). Anal. Calcd: C, 46.14; H, 7.74; N, 21.52. Found: C, 46.04; H, 7.76; N, 21.74.

***N*,*N*-Dimethylpentane Diamide (3a).** The intermediate dimethylamide acid was obtained following Gellman's procedure.[10]

Esterification was performed as for the previous case and afforded the corresponding methyl ester with 69% yield: ^{1}H NMR 200 MHz ($CDCl_3$) δ 1.95 (quintet, 2H, CH_2), 2.37 (t, 2H, CH_2), 2.41 (t, 2H, CH_2), 2.94 (s, 3H, NCH_3), 3.00 (s, 3H, NCH_3), 3.66 (s, 3H, OCH_3). Ammonolysis of the crude ester (1.89 g, 11 mmol) following the general procedure described in Supporting Information afforded 1.22 g (71%) of *N*,*N*-dimethylpentane diamide **2a** as a white solid (Et_2O): mp 102−103 °C; ^{1}H NMR 500 MHz (10 mM, $CDCl_3$) δ 2.01 (quintet, J = 7.0 Hz, 2H, CH_2), 2.37 (t, J = 7.1 Hz, 2H, CH_2), 2.46 (t, J = 6.9 Hz, 2H, CH_2), 2.98 (s, 3H, NCH_3), 3.04 (s, 3H, NCH_3), 5.40 (broad, 1H, NH), 6.10 (broad, 1H, NH). Anal. Calcd: C, 53.15; H, 8.92; N, 17.71. Found: C, 52.85; H, 8.86; N, 17.48.

5-Pentanamide Carboxylic Acid Methyl Ester (4a). Glutaric anhydride (7 g; 61 mmol) was added carefully to 50 mL of NH_3/MeOH 40% at 0 °C. The solution was allowed to warm to room temperature and stirred 2 h. Excess of NH_3/MeOH was eliminated under reduced pressure, and the crude residue was dissolved in 50 mL of MeOH. After cooling the solution to −10 °C, thionyl choride (14.50 g; 122 mmol) in 80 mL of CH_2Cl_2 was added dropwise and stirring was continued for 30 min. After filtration of ammonium chloride, solvents were evaporated. The crude residue was dissolved in CH_2Cl_2/H_2O 50 + 50 mL. The organic layer was dried on Na_2SO_4/K_2CO_3 and evaporated. The crude oil was directly solubilized in Et_2O, which afforded (5.30 g, 60%) of 5-pentanamide carboxylic acid methyl ester **4a** as white microcrystals: mp 87−88 °C; ^{1}H NMR 500 MHz (10 mM, $CDCl_3$) δ 2.00 (quinted, J = 7.2 Hz, 2H, CH_2), 2.33 (t, J = 7.3 Hz, 2H, CH_2), 2.44 (t, J = 7.1 Hz, 2H, CH_2), 3.71 (s, 3H, OCH_3), 5.35 (broad, 1H, NH), 5.50 (broad, 1H, NH). Anal. Calcd: C, 49.65; H, 7.64; N, 9.65. Found: C, 49.38; H, 7.58; N, 9.53.

4-Phenyl Butyramide (5). 4-Phenyl butyric acid was esterified by $SOCl_2$/MeOH with 91% yield. Conversion to 4-phenyl butyramide **5** (83%) was performed following the general ammonolysis procedure described in Supporting Information: mp 83 °C; ^{1}H NMR 500 MHz (10 mM, $CDCl_3$) δ 2.02 (quintet, J = 7.5 Hz, 2H, CH_2), 2.26 (t, J = 7.5 Hz, 2H, CH_2), 2.71 (t, J = 7.5 Hz, 2H, CH_2), 5.35 (broad, 2H, NH_2), 7.21 to 7.33 (m, 5H, aromatics).

Benzylamino Acetamide (6a). Benzylamine (32 g; 300 mmol) and 5.60 g (60 mmol) of chloroacetamide were reacted overnight at room temperature in 100 mL of CH_2Cl_2. Next, 100 mL of 1 M $NaHCO_3$ was added and the mixture was stirred vigorously for 1 h. After evaporation of CH_2Cl_2 the aqueous phase was extracted twice with 50 mL portions of Et_2O, which eliminated around the half (14 g) of the excess of benzylamine. The aqueous phase was then gradually saturated with NaCl until a white solid appeared, which was subsequently removed by filtration. This solid, a benzylamine/benzylamino acetamide (1/1) complex, was dried and dissolved in refluxing CH_2Cl_2. The solution was then reduced to around 50 mL and 150 mL of Et_2O was added. Benzylamino acetamide **6a** crystallized rapidly as colorless needles (5.50 g, 56%): mp 92 °C; ^{1}H NMR 500 MHz (10 mM, $CDCl_3$) δ 3.35 (s, 2H, CH_2), 3.83 (s, 2H, CH_2), 5.45 (broad, 1H, NH), 7.05 (broad, 1H, NH), 7.30 to 7.39 (m, 5H, aromatics). After addition of basic Al_2O_3 in the sample, the amine NH appeared as a broad triplet at 1.83 ppm while signals at 3.35 and 3.83 ppm were doublets (^3J = 5.7 Hz and ^3J = 6.5 Hz, respectively). Anal. Calcd: C, 65.83; H, 7.37; N, 17.06. Found: C, 65.39; H, 7.28; N, 16.87.

Isobutylamino Acetamide (6b). Isobutylamine (11 g; 150 mmol) and 2.80 g (30 mmol) of chloroacetamide were reacted overnight in 50 mL of CH_2Cl_2. Next, 30 mL of 1 M $NaHCO_3$ was added and the mixture was stirred vigorously for 2 h. The organic layer was dried on Na_2SO_4 and evaporation afforded a colorless oil that solidified on standing. This crude compound was dissolved in boiling Et_2O and the solution was cooled by addition of cold pentane, which led rapidly to the crystallization of isobutylamino acetamide **6b** as pearlescent microcrystals (1.91 g, 49%): mp 50−55 °C (waxy); ^{1}H NMR 500 MHz (10 mM, $CDCl_3$) δ 0.96 (d, J = 6.7 Hz, 6H, 2xCH_3), 1.75 (multiplet, J = 6.7 Hz, 1H, CH), 2.47 (d, J = 6.7 Hz, 2H, CH_2), 3.30 (s, 2H, CH_2), 5.40 (broad, 1H, NH), 7.15 (broad, 1H, NH). After addition of basic Al_2O_3 in the sample, the amine NH wasas a broad signal at 1.45 ppm, while the signal at 2.47 ppm was a triplet ($^3J \approx$ 6.5 Hz). Anal. Calcd for **6b**, H_2O: C, 48,64.83; H, 10,81.37; N, 18,91. Found: C, 48,32; H, 10,68; N, 18,74.

Benzylamino Propionamide (7). 3-Chloropropionamide (3.80 g; 35.3 mmol) and benzylamine (18.90 g; 177 mmol) were stirred at room temperature in 100 mL of CH_2Cl_2. Next, 100 mL of 1 M $NaHCO_3$ was added and the mixture was stirred for 24 h. CH_2Cl_2 was evaporated and the aqueous phase was washed with successive 50 mL fractions of an equimolar Et_2O/petroleum ether mixture until no organic material could be further extracted. The aqueous phase was then saturated with NaCl until the appearance of a white suspension, which was extracted twice with 100 mL of CH_2Cl_2. The combined organic layers were dried and reduced to around 50 mL. HCl was then bubbled in CH_2Cl_2. The hydrochloride of compound **7** precipitated as a white powder. The powder was dissolved in 15 mL 1 M $NaHCO_3$. The aqueous phase was saturated with NaCl and extracted twice with 20 mL of EtOAc. Drying of the organic phase on Na_2SO_3 and evaporation afforded **7** as a white powder, which was filtrated after trituration in Et_2O (1.67 g, 26.6%): mp 96 °C; ^{1}H NMR 500 MHz (10 mM, $CDCl_3$) δ 2.43 (t, J = 5.9 Hz, 2H, CH_2), 2.95 (t, J = 5.9 Hz, 2H, CH_2), 3.84 (s, 2H, CH_2), 5.35 (broad, 1H, NH), 7.30 to 7.38 (m, 5H, aromatics), 7.50 (broad, 1H, NH). Anal. Calcd: C, 67.42; H, 7.87; N, 15.73. Found: C, 67.27; H, 7.70; N, 15.55.

(Benzyl,*tert*-butoxycarbonyl-methyl) Amino Acetamide (8a). Benzylamino acetamide **6a** (1.64 g, 10 mmol) and 1.10 g (5.5 mmol) of tertiobutyl bromoacetate were stirred in 30 mL of CH_2Cl_2 for 20 h. **6a**, HBr was filtrated. The organic layer was washed with 20 mL of 1 M $NaHCO_3$, dried, and evaporated. The residue was triturated in petroleum ether to give **8a** as white amorphous powder (1.20 g, 86%): mp 90−92 °C; ^{1}H NMR 500 MHz (10 mM, $CDCl_3$) δ 1.48 (s, 9H, 3xCH_3), 3.30 (s, 2H, CH_2), 3.31 (s, 2H, CH_2), 3.83 (s, 2H, CH_2), 5.45 (broad, 1H, NH), 7.30 to 7.38 (m, 5H, aromatics), 7.55 (broad, 1H, NH). Anal. Calcd: C, 64.73; H, 7.97; N, 10.06. Found: C, 65.06; H, 8.03; N, 10.17.

(Benzyl,dimethylaminocarbamoyl-methyl) Amino Acetamide (8b). Benzylamino acetamide **6a** (1.64 g; 10 mmol) and 0.84 g (5.5 mmol) of methyl bromoacetate were stirred in 30 mL of CH_2Cl_2 for 20 h. **6a**, HBr was filtrated. The organic layer was washed with 20 mL of 1 M $NaHCO_3$, dried, and evaporated. Trituration of the residue in 30 mL of Et_2O afforded (benzyl,methoxycarbonyl-methyl) amino acetamide as a white amorphous powder: mp 91 °C; ^{1}H NMR 200 MHz (10 mM, $CDCl_3$) δ 3.30 (s, 2H, CH_2), 3.40 (s, 2H, CH_2), 3.73 (s, 3H, OCH_3), 3.81 (s, 2H, CH_2), 5.45 (broad, 1H, NH), 7.30 to 7.45 (m, 5H, aromatics), 7.45 (broad, 1H, NH).

This solid was directly poured into 40 mL of dimethylamine 40 wt % solution in water, 0.027 g of NaCN (0.55 mmol) was added, and the mixture was stirred for 3 days at room temperature. The solution was reduced to around 5 mL, saturated with NaCl, and extracted twice with 30 mL of CH_2Cl_2. After drying over Na_2SO_4, evaporation yielded a thick oil, which was dissolved in EtOAc /Et_2O (1/5). **8b** slowly precipitated as white globular colonies (0.76 g, 55% for the two steps): mp 105−110 °C (waxy fusion); ^{1}H NMR 500 MHz (10 mM, $CDCl_3$) δ 2.89 (s, 3H, NCH_3), 2.96 (s, 3H, NCH_3), 3.33 (s, 2H, CH_2), 3.42 (s, 2H, CH_2), 3.83 (s, 2H, CH_2), 5.45 (broad, 1H, NH), 7.29 to 7.37 (m, 5H, aromatics), 8.05 (broad, 1H, NH). Anal. Calcd: C, 62.63; H, 7.68; N, 16.85. Found: C, 62.61; H, 7.61; N, 16.79.

(Dicarbamoyl-methyl) Benzylamine (**8c).** Compound **8c** was prepared following the same procedure as **8b** except that the final step was the general ammonolysis procedure described in Supporting Information (78%): mp (EtOAc) 157 °C; ^{1}H NMR 200 MHz (10 mM, $CDCl_3$) δ 3.30 (s, 4H, 2 × CH_2), 3.82 (s, 2H, CH_2), 5.45 (broad, 2H, 2 × NH), 6.65 (broad, 2H, 2 × NH), 7.30 to 7.45 (m, 5H, aromatics). Anal. Calcd: C, 64.73; H, 7.97; N, 10.06. Found: C, 65.06; H, 8.03; N, 10.17.

***N*$^{\alpha}$-2-Pyridylmethyl,*N*$^{\beta}$-Boc Hydrazino Acetamide (9).** 2-Pyridine-carboxaldehyde (10 g; 93 mmol) and 12.34 g of tertiobutylcarbazate (93 mmol) were stirred for 12 h in 100 mL of ether in the presence of excess of Na_2SO_4. After filtration of the drying agent, the solvent was evaporated and the resulting hydrazone, filtrated as a white powder using Et_2O, was dried under vacuum (20.55 g, 92%): mp 148−150 °C; ^{1}H NMR 200 MHz ($CDCl_3$) δ 1.58 (s, 9H, 3xCH_3), 7.29 (dd, J = 7 Hz, J = 5 Hz, 1H, CH), 7.73 (td, J = 7 Hz, J = 2 Hz, 1H, CH), 7.95 (s, 1H, CH), 8.11 (d, J = 7 Hz, 1H, CH), 8.25 (broad, 1H, NH), 8.60 (dd, J = 5 Hz, J = 2 Hz, 1H, CH). The hydrazone, dissolved in 100 mL of 2-propanol, was hydrogenated quantitatively at atmospheric pressure in the presence of 500 mg of 10% Pd/C. After 48 h, the solution was filtrated on Celite and evaporated to give the corresponding hydrazine as a colorless oil that solidified on cooling: mp 118−120 °C; ^{1}H NMR 200 MHz ($CDCl_3$) δ 1.44 (s, 9H, 3xCH_3), 4.13 (s, 2H, CH_2), 4.55 (broad, 1H, NH), 6.40 (broad, 1H, NH), 7.18 (dd, J = 7 Hz, J = 5 Hz, 1H, CH), 7.27 (d, J = 7 Hz, 1H, CH), 7.62 (td, J = 7 Hz, J = 2 Hz, 1H, CH), 8.62 (dd, J = 5 Hz, J = 2 Hz, 1H, CH). Next, 15 g of this hydrazine (72 mmol) was dissolved in 50 mL of MeOH. After addition of 9.95 g of glyoxylic acid monohydrate (108 mmol) and cooling at 5 °C, 6.80 g of $NaBH_3CN$ (108 mmol) was added. After 20 h of stirring, the pH was adjusted to 1 using 1 N HCl. The MeOH was evaporated and cooled to 5 °C. The pH was adjusted to around 4 by progressively adding solid $NaHCO_3$. At this value, a brown oil was eliminated using CH_2Cl_2. The pH was then adjusted to 5.5 and the solution was saturated with NaCl. Extraction with twice 50 mL of CH_2Cl_2, drying on Na_2SO_4 and evaporation afforded *N*$^{\alpha}$-2-pyridylmethyl,*N*$^{\beta}$-Boc hydrazino acetic acid as an off-white powder (12 g, 59%): mp 136−138 °C; ^{1}H NMR 200 MHz ($CDCl_3$) δ 1.42 (s, 9H, 3xCH_3), 3.73 (s, 2H, CH_2), 4.39 (s, 2H, CH_2), 6.35 (broad, 3H, OH, H_2O), 7.37 (dd, J = 7 Hz, J = 5 Hz, 1H, CH), 7.56 (broad, 1H, NH), 7.70 (d, J = 7 Hz, 1H, CH), 7.86 (td, J = 7 Hz, J = 2 Hz, 1H, CH), 8.60 (dd, J = 5 Hz, J = 2 Hz, 1H, CH). The acid (1 g; 3.56 mmol) and DCC (0.734 g; 3.56 mmol) were dissolved in 20 mL of MeOH and stirred for 3 h. The solvent was eliminated and replaced by 20 mL of Et_2O. Filtration of DCU and evaporation afforded the corresponding ester as an oil that solidified slowly on standing. The final amide **9** was obtained using the general ammonolysis procedure described in Supporting Information. Both steps were quantitative: mp (EtOAc) 144−145 °C; ^{1}H NMR 500 MHz (10 mM, $CDCl_3$) δ 1.44 (s, 9H, 3xCH_3), 3.51 (s, 2H, CH_2), 4.21 (s, 2H, CH_2), 5.45 (broad, 1H, NH), 7.26 (dd, J = 7.3 Hz, J = 5.1 Hz, 1H, CH), 7.31 (d, J = 8.1 Hz, 1H, CH), 7.41 (broad, 1H, carbazidic NH), 7.71 (t, J = 7.7 Hz, 1H, CH) 8.35 (broad, 1H, NH), 8.59 (d, J = 5.0 Hz, 1H, CH). Anal. Calcd: C, 55.70; H, 7.19; N, 19,99. Found: C, 55.56; H, 7.20; N, 19.95.

Supporting Information Available: Characterization data for compounds **1a**, **1b**, **1c**, **2a**, **3a**, **4a**, **5**, **6a**, **6b**, **7**, **8a**, **8b**, **8c**, and **9**; copies of ^{1}H NMR spectroscopic data; superposition of ^{1}H NMR spectra at different concentrations in $CDCl_3$ (from 10 mM to 100 mM) for compound **2a** and **3a**; superposition of ^{1}H NMR spectra ($CDCl_3$) in the presence of increasing amount of DMSO (0−9%) for compound **2a** and **3a**; graphics showing the variation of the chemical shifts of NHs as a function of the concentration of DMSO-d_6 in $CDCl_3$ (0−9%) for compounds **1a**, **6b**, and **8a**; portions of the 2D NOESY spectrum and the summary of NOEs observed for compound **1a** in $CDCl_3$ at room temperature (s, strong NOE; m, medium NOE); crystallographic data in CIF format for compounds **1a** and **6a**; general ammonolysis procedure. This material is available free of charge via the Internet at http://pubs.acs.org.

JO051887Q